Computational Density Functional Theory Investigation of Stability and Electronic Structures on Boron Nitride Systems Doped with/without Group IV Elements

Syed Amir Abbas Shah Naqvi[1], Pek-Lan Toh[1]*, Yao-Cong Lim[1], Suh-Miin Wang[1], Lee-Sin Ang[2] and Lan-Ching Sim[3]

[1]Faculty of Engineering and Green Technology, Universiti Tunku Abdul Rahman, 31900 Kampar, Malaysia

[2]Fakulti Sains Gunaan, Universiti Teknologi MARA Cawangan Perlis, Malaysia

[3]Lee Kong Chian, Faculty of Engineering and Science, Universiti Tunku Abdul Rahman, 43200 Kajang, Malaysia

*Corresponding author (e-mail: tohpl@utar.edu.my)

In this paper, the stability as well as electronic structures of pure and group IV-substituted boron nitride (BN) cluster systems were investigated using Density Functional Theory (DFT) method. The results obtained from the DFT calculations found that the germanium-substituted BN model possessed the highest stability among all the group IV-substituted BN clusters. Although the energy gap values calculated were slightly different for all group IV-substituted single-layered BN clusters, the surface plots of HOMO and LUMO obtained were still the same. For the plots of molecular electrostatic potentials (MEPs), the nitrogen atom located in the middle of the pure BN system has the most negative electrostatic potentials. In the case of the group IV-substituted BN models, three atoms (i.e., carbon, silicon, and germanium) presented the most reactive sites for nucleophilic attack on the cluster systems. Mulliken atomic charges reported a similar trend as observed in MEPs. In the Mulliken scheme, the nitrogen atom located in the middle of the pure BN system possesses the highest negative charge. While three atoms (i.e., carbon, silicon, and germanium) showed the highest negative charges in the group IV-substituted BN model clusters.

Boron nitride was introduced as a hydrogen storage material in recent years. Lale *et al.* studied the physisorption and chemisorption of hydrogen in BN system using a large temperature range of -160°C to 300°C [1]. Tabtimsai *et al.* studied the interactions of metal atoms with hydrogen atoms, which is a primary interest of scientists working on energy storage materials around the globe [2]. As far as we know hydrogen is omnipresent and found rarely in the pure gaseous form in particular conditions. It has a high energy density and a well-known secondary source of energy for modern automobiles. It can compensate the natural fuel efficiently results in green and cleaner energy solutions [3]. In the world of catalysis and energy storage materials, interactions of geometric sites of substrates are the keen interest of recent scientists [4]. Atomic H_2 reacts readily with lighter metals; lithium, sodium, magnesium etc., to form hydrides; since these metals are of the prime choice for hydrogen storage materials, the molecule of H_2 is under investigation for both adsorption and absorption on these metals [5, 6]. Contrary to this, the 3*d*, 4*d*, and 5*d* metals from *d* and *f* blocks are under study for low-cost green manufacturing chemical processes [7]. In 2004, Jhi and
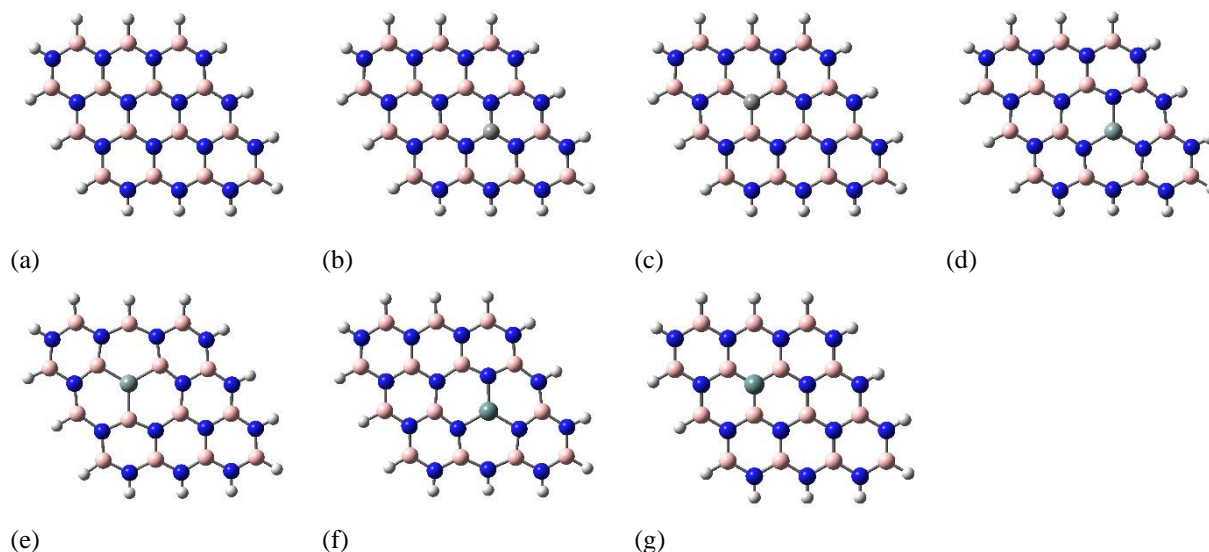
Kwon carried out theoretical studies that showed hexagonal BN (h-BN) is the best 2D material for H_2 storage, even better than graphene [8]. In 2007, Mpourmpakis and Froudak reported carbon nanotubes (CNTs) having 0.2 wt% hydrogen storage capacity (HSC), while BN nanotubes (BNNTs) have 3 wt% HSC, which is marginally greater than carbon nanotubes H storage capacity [9]. This is because B-N bonding is heteropolar, which is promising to bind H_2 strongly with C-C from other materials, which have nonpolar nature. Moreover, there are more advanced and novice techniques of modifying edges, spacing of interlayers, wrinkling processes, doping by heteroatoms, protrusion process, vacancies for adsorption, creating geometric sites, and foreign metal decorating are under exploration [4]. These are not restricted to other hydrogen storage materials (HSMs), but BN is also one of the competitive candidates for these technologies in recent years [10]. In 2012, Zhang and his co-workers applied computational DFT methods to study BNNTs decorated by Ce particles [11]. Unfortunately, such interactions of hydrogen to metal-adsorbed atoms and geometry aspects of adatom substrates have not been verified nor understood completely in the study.

86   Syed Amir Abbas Shah Naqvi, Pek-Lan Toh,
      Yao-Cong Lim, Suh-Miin Wang, Lee-Sin Ang
      and Lan-Ching Sim

Computational Density Functional Theory Investigation
of Stability and Electronic Structures on Boron Nitride
Systems Doped with/without Group IV Elements

Many experts have used the term "Hydrogen Economy" as hydrogen has become the most reliable and promising source of energy in the emerging energy crises of the world [1, 12]. There is a combined quest for its three aspects, namely storage, production, and final usage [13, 14]. However, for researchers, there are certain technological and technical difficulties. The major approaches include both the classical and modern methods that can be used to overcome these issues. In the light of classical gas laws, researchers reported storing its maximum volume by decreasing the temperature up to -253°C and applying the high pressure of 700 to 800 bars [15, 16]. This method is termed as physical storage of H_2. From the literature studies, the novel approaches use microporous and sorbent polymers, such as metal-organic framework (MOF), magnesium and aluminium metallic hydrides, boron hydrides, organic hydrogen carriers, and metal-N-H system [17]. Sorbents can be used at cryogenic conditions due to the maximum reversible H_2 storage capacity [18]. This is also classified in the physical methods for H_2 storage. For example $Zn_4O(BDC)_3$, where BDC (1,4-benzenedicarboxylate) has the surface area of almost 3800 $m^2 g^{-1}$, and has 7.1% of hydrogen at 40 bars of hydrogen and -196°C [19]. When hydrogen storage materials are compared to each other, results clearly show that boranes and borohydrides can release and store H_2 at 20-100°C and ambient conditions. Also, their H_2 carrying capacity is very low. In addition, this process can also be called the chemical storage of H_2 [20]. NH_3BH_3 (pristine ammonia one) undergoes dehydrogenation at 100°C, whereas if it is modified chemically to lithium amidoborane ($LiNH_2BH_3$), then it releases 10% of H_2 at 90°C [21, 22, 23]. Both $LiNH_2BH_3$ and NH_3BH_3 can be called B- and N-based hydrogen storage materials in this study. BN was first introduced as a H_2 storage substance [24]. It has many reliable characteristics like when milled at 10 bars its 3 nm crystals were able to carry H_2. It was further reported that this uptake capacity increased from 0.5 wt% to 2.6 wt% when the milling time was increased from 5 h to 80 h. The highest value of H_2 uptake was recorded at -196°C and 10 bars of pressure. Its active surface area was 1144 $m^2 g^{-1}$. Shahsavari and Zhao, in 2018, studied the largest storage of H_2 of about 19.3 wt% at -196°C and

100 bars of pressure in the nano and pillared forms of BN [25]. One of the important parameters for hydrogen storing capacity is pore width [26]. For example, Weng *et al.* studied highly porous BN (i.e., BN in spongy shape) that has a pore width of 1 nm and reversible storage capacity of 2.57 wt% hydrogen at -196°C and 10 bars of pressure [26]. Another important parameter for the storage of hydrogen is surface area [27]. In 2002, Ma *et al.* reported the comparison between bamboo-like BN nanotubes and multiwalled BN nanotubes. In addition, the hydrogen storage was also recorded at 20°C and 100 bars, where the former had the capacity of 2.6 wt%, while the later 1.8 wt% [28]. From the literature studies, BN nanostructures are more suitable for H_2 storage due to their BN ionic characteristics, which result in the higher binding energy of H_2 [29]. In 2007, Cheng *et al.* presented H_2 uptake greater than 6 wt% obtained at 100 bars and 20°C for single-walled BN nanotubes having 30 nm diameter [30]. There are prime applications of metallic atoms and H_2 interactions for energy processing systems, particularly H_2 storage purposes using catalytic approaches. There are not many literature studies on BN systems via the computational DFT technique. In this paper, we conducted the DFT method to study the stability and electronic structures on pure, carbon, silicon, and germanium-substituted BN monolayers.

COMPUTATIONAL METHODOLOGY

In this study, the computational DFT technique was used to study the electronic structures of pure and group IV-substituted single-layered BN using Gaussian 09 software program [31]. First, the cluster structures of (3,3) BN cluster models were chosen as the host environment. Figure 1 illustrates the cluster structures of pure and group IV-substituted single-layered BN. All BN model clusters were fully optimized using geometry optimization calculations at the B3LYP/6-31++G** level of theory. The equilibrium structures of the BN systems were then used to determine the local energy minima. Moreover, the electronic parameters such as Frontier molecular orbitals (FMOs), MEP surface, and Mulliken atomic charges were calculated by employing single point calculations.

87   Syed Amir Abbas Shah Naqvi, Pek-Lan Toh,
     Yao-Cong Lim, Suh-Miin Wang, Lee-Sin Ang
     and Lan-Ching Sim

Computational Density Functional Theory Investigation
of Stability and Electronic Structures on Boron Nitride
Systems Doped with/without Group IV Elements

Figure 1. Optimized structure models of (a) pure, (b) C_B, (c) C_N, (d) Si_B, (e) Si_N, (f) Ge_B, and (g) Ge_N-substituted boron nitride monolayers, where hydrogen (white), nitrogen (blue), boron (pink), carbon (grey), silicon (blue grey), and germanium (green grey).

RESULTS AND DISCUSSION

For all equilibrium structures of the BN models, all optimized B-N bond distances were determined in the range of 1.42 Å – 1.46 Å. The results obtained are close to literature data [32]. Moreover, the computed bond distances of B-H and N-H were 1.19 Å and 1.01 Å, respectively, in the studied BN systems. Table 1 shows the total energies of pure, carbon, silicon, and germanium-substituted monolayer BN. As we know, computed total energy depends on cluster size selected, as well as configuration atoms used in the study. From the table, the total energy of pure boron nitride was calculated to be -31767.096 eV. For carbon-substituted single-layered BN, the total energies obtained were from -33122.783 eV to -32309.886 eV. Also, the computed total energies of silicon-substituted boron nitride were between 39963.179 eV and -39145.824 eV. While for germanium-substituted monolayer BN, the calculated total energies obtained were in the range from -88549.795 eV to -87733.192 eV. The ground state of the model system is the minimum total energy curve in the molecular system. In this study, the total energy obtained could be used to explain the stability of the cluster system. Overall, it could be found that $B_{15}N_{14}GeH_{14}$ is the stable one as compared to the other systems because the total energy of $B_{15}N_{14}GeH_{14}$ was the lowest. From the literature studies, Frontier molecular orbital plays important roles in the studies of molecular interactions and chemical reactivity in the systems [33-36]. In Table 1, the results of Frontier molecular orbital energies of pure, carbon, silicon, and germanium-substituted monolayer BN are also presented. The HOMO-LUMO energy of pure BN was 6.201 eV, whereas, for carbon, silicon, and germanium-substituted monolayer BN, the computed HOMO-LUMO energy values were from 1.310 eV to 5.883 eV. In addition, these HOMO-LUMO gaps obtained from the DFT calculations could also be used to indicate chemical stability in the BN cluster models [33-36]. For example, the larger the HOMO-LUMO energy gap obtained, the higher the hardness and the chemical stability of the system presented in the table. While the smaller HOMO-LUMO energy gaps mean the easier electrons are excited in the BN model systems. The calculated results obtained are in reasonable agreement with the literature data [33-36]. From the table, it can be noted that the HOMO-LUMO energy of pure BN was the highest if compared to the other cluster systems. While for $B_{14}N_{15}SiH_{14}$, the HOMO-LUMO gap was the lowest in this study.

88   Syed Amir Abbas Shah Naqvi, Pek-Lan Toh,
     Yao-Cong Lim, Suh-Miin Wang, Lee-Sin Ang
     and Lan-Ching Sim

Computational Density Functional Theory Investigation
of Stability and Electronic Structures on Boron Nitride
Systems Doped with/without Group IV Elements

Table 1. Total and Frontier molecular orbital energies (eV) of pure, carbon, silicon, and germanium-substituted monolayer boron nitride.

	$B_{15}N_{15}H_{14}$	$B_{14}N_{15}CH_{14}$	$B_{15}N_{14}CH_{14}$	$B_{14}N_{15}SiH_{14}$	$B_{15}N_{14}SiH_{14}$	$B_{14}N_{15}GeH_{14}$	$B_{15}N_{14}GeH_{14}$
Total Energy	-32767.096	-33122.783	-32309.886	-39963.179	-39145.824	-88549.795	-87733.192
HOMO	-6.810	-2.915	-6.503	-2.304	-4.886	-2.428	-4.865
LUMO	-0.609	-0.621	-0.620	-0.994	-0.918	-0.951	-0.933
Ionization potential (IP)	6.810	2.915	6.503	2.304	4.886	2.428	4.865
Electron Affinity (EA)	0.609	0.621	0.620	0.994	0.918	0.951	0.933
Chemical Potential (CP)	-3.710	-1.768	-3.562	-1.649	-2.902	-1.690	-2.899
Global Hardness (GP)	3.101	1.147	2.942	0.655	1.984	0.739	1.966
Electronegativity (EN)	3.710	1.768	3.562	1.649	2.902	1.690	2.899
Electrophilicity (EP)	2.219	1.363	2.156	2.076	2.122	1.933	2.137
Softness (S)	0.323	0.872	0.340	1.527	0.504	1.354	0.509
HOMO-LUMO Energy	6.201	2.294	5.883	1.310	3.967	1.477	3.932

Table 2 illustrates the diagrams of Frontier molecular orbital distributions for pure, carbon, silicon, and germanium-substituted monolayer BN in this study. From the table, it can be found that there were two different views, i.e., top and side views, for HOMO and LUMO for pure, carbon, silicon, and germanium-substituted BN. These HOMO and LUMO diagrams clearly showed the electron distributions of the BN model systems in this study. The red and green surfaces indicated the positive and negative phases in the BN systems. Therefore, it could be noted that for the HOMO of pure BN, the electron distribution was localized on nitrogen atoms. In the case of the HOMO surface plots, carbon, silicon, and germanium-substituted monolayer BN were close to each other. While the LUMO surface plots of carbon-substituted BN were similar to the pure boron nitride. The surface plots of LUMO for silicon and germanium-substituted BN were the same in this study.
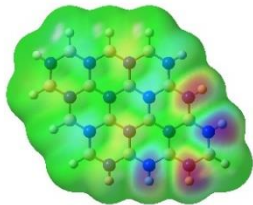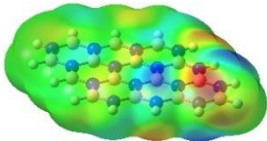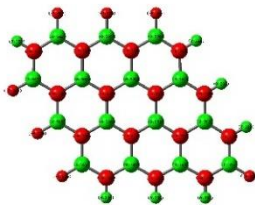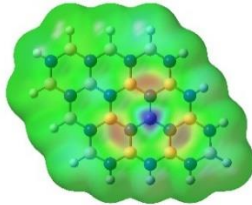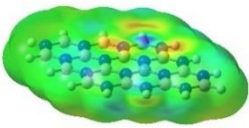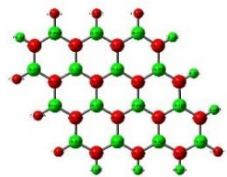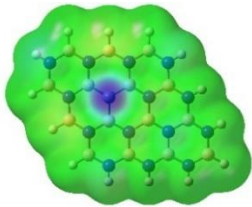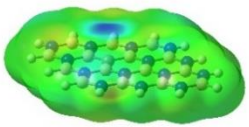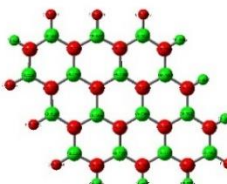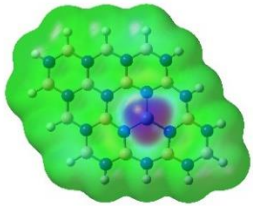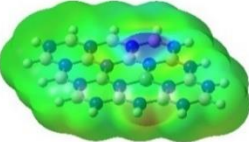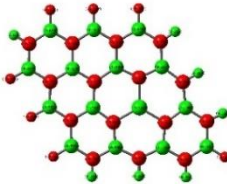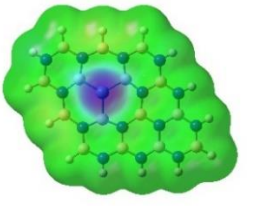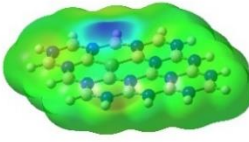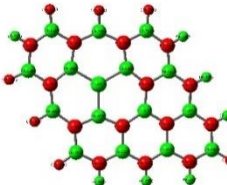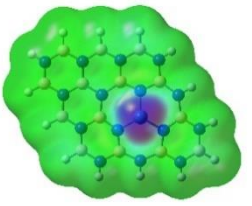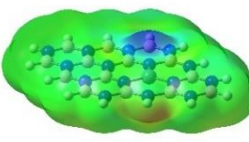
The molecular electrostatic potential surface maps and Mulliken atomic charge distributions of pure, carbon, silicon, and germanium-substituted BN are illustrated in Table 3. From the table, it can be found that there were two different views, i.e., top and side views, for electrostatic potential surface maps for pure, carbon, silicon, and germanium-substituted BN. Also, the top view of Mulliken atomic charge distributions for pure, carbon, silicon, and germanium-substituted boron nitride is

presented in this study. From the literature studies, the study of molecular electrostatic potential is one of useful tools that helps to study how a molecular system interacts with its surroundings [36]. In this work, the molecular electrostatic potential surface map provides useful information about the charge distribution in the title system. As can be seem from the diagrams obtained in Table 3, the surface maps were coloued according to the local electrostatic potential in the title system, such as blue, green, yellow, and red. From the computed electrostatic potential maps, it could be found that the blue surface showed the most positive electrostatic potential, whereas the most negative electrostatic potential was presented in the region of the red surface. For pure boron nitride, the nitrogen atom at the center possessed the most negative electrostatic potentials, whereas the most positive electrostatic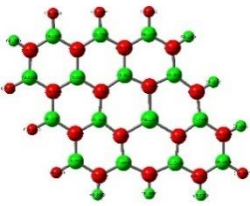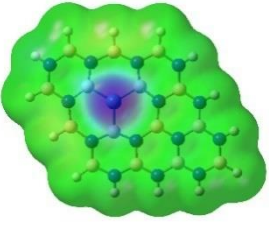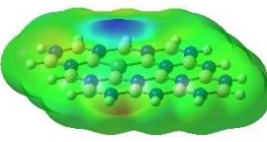 potentials were focused on H atoms at N-edges in this study. For the group IV-substituted BN clusters, the most positive electrostatic potentials were localized on the carbon, silicon, and germanium atoms. The results noted that all group IV atoms are the most reactive for nucleophilic attack in the title systems. Similar results were obtained on the Mulliken atomic charge distributions. The highest negative charges were found on the carbon, silicon, and germanium atoms for the cluster systems of carbon, silicon, and germanium-substituted BN, respectively.

89 Syed Amir Abbas Shah Naqvi, Pek-Lan Toh,
Yao-Cong Lim, Suh-Miin Wang, Lee-Sin Ang
and Lan-Ching Sim

Computational Density Functional Theory Investigation
of Stability and Electronic Structures on Boron Nitride
Systems Doped with/without Group IV Elements

Table 2. Frontier molecular orbital distributions of pure, carbon, silicon, and germanium-substituted monolayer boron nitride.

	HOMO		LUMO	
	Top	Side	Top	Side
$B_{15}N_{15}H_{14}$				
$B_{14}N_{15}CH_{14}$				
$B_{15}N_{14}CH_{14}$				
$B_{14}N_{15}SiH_{14}$				
$B_{15}N_{14}SiH_{14}$				
$B_{14}N_{15}GeH_{14}$				
$B_{15}N_{14}GeH_{14}$				

90   Syed Amir Abbas Shah Naqvi, Pek-Lan Toh,
     Yao-Cong Lim, Suh-Miin Wang, Lee-Sin Ang
     and Lan-Ching Sim

Computational Density Functional Theory Investigation
of Stability and Electronic Structures on Boron Nitride
Systems Doped with/without Group IV Elements

Table 3. Molecular electrostatic potential surface maps and Mulliken atomic charges of pure, carbon, silicon, and germanium-substituted monolayer boron nitride.

	Molecular Electrostatic Potentials		Mulliken Atomic Charges
	Top	Side	
$B_{15}N_{15}H_{14}$			
$B_{14}N_{15}CH_{14}$			
$B_{15}N_{14}CH_{14}$			
$B_{14}N_{15}SiH_{14}$			
$B_{15}N_{14}SiH_{14}$			
$B_{14}N_{15}GeH_{14}$			
$B_{15}N_{14}GeH_{14}$			

91   Syed Amir Abbas Shah Naqvi, Pek-Lan Toh,
      Yao-Cong Lim, Suh-Miin Wang, Lee-Sin Ang
      and Lan-Ching Sim

Computational Density Functional Theory Investigation
of Stability and Electronic Structures on Boron Nitride
Systems Doped with/without Group IV Elements

CONCLUSIONS

In this study, the optimized structures of BN cluster models were used to determine the total energies and other electronic properties by employing the DFT/B3LYP/6-31++G** level of theory. According to the findings obtained from the DFT calculations, $B_{15}N_{14}GeH_{14}$ possessed the lowest energy among all BN cluster models. It was revealed that the relative stability of the $B_{15}N_{14}GeH_{14}$ molecule is the highest compared to other BN cluster models. For HOMO and LUMO surface plots, the group IV-substituted monolayer BN were close to each other, while the electron distribution of pure BN was slightly different. Moreover, for the pure BN model, the nitrogen atom at the center clearly showed the most negative electrostatic potentials. While the most reactive to nucleophilic attacks on the group IV-substituted BN model systems were carbon, silicon, and germanium atoms. The same results were presented on the distributions of Mulliken atomic charges. For example, carbon, silicon, and germanium atoms possessed the highest negative charges in the group IV-substituted BN clusters, whereas the highest negative charge was obtained on the nitrogen atom at the center of the pure BN cluster system. We believe that our DFT investigations in this study could be valuable for the BN nanosheet for hydrogen molecule storage in future studies.

ACKNOWLEDGMENTS

REFERENCES

1.   Lale, A., Bernard, S. and Demirci, U. B. (2018) Cover Feature: Boron Nitride for Hydrogen Storage. *ChemPlusChem*, **83(10)**, 888.

2.   Tabtimsai, C., Ruangpornvisuti, V., Tontapha, S. and Banchob, W. (2018) A DFT investigation on group 8B transition metal-doped silicon carbide nanotubes for hydrogen storage application. *Applied Surface Science*, **439**, 494–505.

3.   Choudhary, A., Malakkal, L., Siripurapu, K. R., Szpunar, B. and Szpunar, J. (2016) First principles calculations of hydrogen storage on Cu and Pd-decorated graphene. *International Journal of Hydrogen Energy*, **41(39)**, 17652–17656.

4.   Yang, Y., Liu, X., Zhu, Z., Zhong, Y., Bando, Y., Golberg, D., Yao, J. and Wang, X. (2018) The Role of Geometric Sites in 2D Materials for Energy Storage. *Joule*, **2(6)**, 1075–1094.

5.   Li, Q. -F., Wan, G. X., Duan, G. -C. and Kuo, L. -J. (2014) Theoretical prediction of hydrogen storage on Li-decorated monolayer black phosphorus. *Journal of Physics D: Applied Physics*, **47(46)**, 465302.

6.   Luo, Q., Li, J., Li, B., Liu, B., Shao, H. and Li, Q. (2019) Kinetics in Mg-based hydrogen storage materials: Enhancement and mechanism. *Journal of Magnesium and Alloys*, **7(1)**, 58–71.

7.   Egorova, K. S. and Ananikov, V. P. (2016) Which Metals are Green for Catalysis? Comparison of the Toxicities of Ni, Cu, Fe, Pd, Pt, Rh, and Au Salts. *Angewandte Chemie International Edition*, **55(40)**, 12150–12162.

8.   Jhi, S. -H. and Kwon, Y. -K. (2004) Hydrogen adsorption on boron nitride nanotubes: A path to room-temperature hydrogen storage. *Physical Review B*, **69(24)**, 245407.

9.   Mpourmpakis, G. and Froudakis, G. E. (2007) Why boron nitride nanotubes are preferable to carbon nanotubes for hydrogen storage?: An ab initio theoretical study. *Catalysis Today*, **120(3)**, 341–345.

10.   Samolia, M. and Kumar, T. J. D. (2014) A conceptual DFT study of the hydrogen trapping efficiency in metal functionalized BN system. *RSC Advances*, **4(58)**, 30758–30767.

11.   Zhang, Z. -W., Zheng, W. -T. and Jiang, Q. (2012) Hydrogen adsorption on Ce/BNNT systems: A DFT study. *International Journal of Hydrogen Energy*, **37(6)**, 5090–5099.

12.   Bockris, J. O. M. (1999) Hydrogen economy in the future fn2. *International Journal of Hydrogen Energy*, **24(1)**, 1–15.

13.   Marbán, G. and Valdés-Solís, T. (2008) Corrigendum to "Towards the hydrogen economy?" [Int. J. Hyd. Energy 32(12) (2007) 1625–1637]. *International Journal of Hydrogen Energy*, **33(2)**, 927.

14.   Braga, B. L., Silva, d. E. M., Colombaroli, S. T., Tuna, E. C., Araujo, d. M. H. F., Vane, F. L., Pedroso, T. D. and Silveira, L. J. (2017) Hydrogen Production Processes, in Silveira J. (eds) Sustainable Hydrogen Production Processes. *Green Energy and Technology, Springer, Cham*, 5–76.

15.   Klebanoff, L. (Ed.). (2012) Hydrogen Storage

92 Syed Amir Abbas Shah Naqvi, Pek-Lan Toh,
Yao-Cong Lim, Suh-Miin Wang, Lee-Sin Ang
and Lan-Ching Sim

Computational Density Functional Theory Investigation
of Stability and Electronic Structures on Boron Nitride
Systems Doped with/without Group IV Elements

Technology: Materials and Applications (1st Edition), *CRC Press*.

16. Weinheim, W. -V. (2012) Fuel Cells: Problems and Solutions (Second Edition (Ed.: Bagotsky, V. S.).

17. Chamoun, R., Demirci, U. B. and Miele, P. (2015) Cyclic Dehydrogenation–(Re)Hydrogenation with Hydrogen-Storage Materials: An Overview. *Energy Technology*, **3(2)**, 100−117.

18. Bhatia, S. K. and Myers, A. L. (2006) Optimum Conditions for Adsorptive Storage. *Langmuir*, **22(4)**, 1688−1700.

19. Kaye, S. S., Dailly, A., Yaghi, M. O. and Long, R. J. (2007) Impact of preparation and handling on the hydrogen storage properties of Zn4O(1,4-benzenedicarboxylate)3 (MOF-5). *J Am Chem Soc*, **129(46)**, 14176−7.

20. Demirci, U. B. (2018) About the Technological Readiness of the H2 Generation by Hydrolysis of B(−N)−H Compounds. *Energy Technology,* **6(3)**, 470–486.

21. Petit, J.-F., Gaveau, P. D. E., Miele, P., Alonso, B. and Demirci, B. U. (2017) ^{11}B MAS NMR Study of the Thermolytic Dehydrocoupling of Two Ammonia Boranes upon the Release of One Equivalent of H_2 at Isothermal Conditions, ChemistrySelect, **2(29)**, 9396−9401.

22. Hu, X.-B., Chen, Z., Chen, L., Zhang, L., Hou, L.-J. and Li, T.-Z. (2012) Pillar[n]arenes (n = 8–10) with two cavities: synthesis, structures and complexing properties, Chemical Communications, **48(89)**, 10999−11001.

23. Zhu, Y., Gao, S. and Hosmane, N. S. (2018) Boron-enriched advanced energy materials, Inorg. Chim. Acta 2018, **471**, 577−586.

24. Wang, P., Orimo, S., Matsushima, T. and Fujii, H. (2002) Hydrogen in mechanically prepared nanostructured h-BN: a critical comparison with that in nanostructured graphite, Applied Physics Letters, **80(2)**, 318−320.

25. Shahsavari, R. and Zhao, S. (2018) Merger of Energetic Affinity and Optimal Geometry Provides New Class of Boron Nitride Based Sorbents with Unprecedented Hydrogen Storage Capacity, Small, **14(15)**, 1702863.

26. Weng, Q., Wang, X., Bando, Y. and Golberg, D. (2014) One-Step Template-Free Synthesis of Highly Porous Boron Nitride Microsponges for Hydrogen Storage, Advanced Energy Materials, **4(7)**, 1301525.

27. Ma, R., Bando, Y., Zhu, H., Sato, T., Xu, C. and Wu, D. (2002) Hydrogen Uptake in Boron Nitride Nanotubes at Room Temperature, Journal of the American Chemical Society, **124(26)**, 7672−7673.

28. Reddy, A. L. M., Tanur, A. E. and Walker, G. C. (2010) Synthesis and hydrogen storage properties of different types of boron nitride nanostructures, International Journal of Hydrogen Energy, **35(9)**, 4138−4143.

29. Fendley, P., Sengupta, K. and Sachdev, S. (2004) Competing density-wave orders in a one-dimensional hard-boson model, Physical Review B, **69(7)**, 075106.

30. Cheng, J., Zhang, L., Ding, R., Ding, Z., Wang, X. and Wang, Z. (2007) Grand canonical Monte Carlo simulation of hydrogen physisorption in single-walled boron nitride nanotubes. *International Journal of Hydrogen Energy*, **32(15)**, 3402−3405.

31. Frisch, M. J., Trucks, G. W., Schlegel, H. B., Scuseria, G. E., Robb, M. A., Cheeseman, J. R., Scalmani, G., Barone, V., Mennucci, B., Petersson, G. A., Nakatsuji, H., Caricato, M., Li, X., Hratchian, H. P., Izmaylov, A. F., Bloino, J., Zheng, G., Sonnenberg, J. L., Hada, M., Ehara, M., Toyota, K., Fukuda, R., Hasegawa, J., Ishida, M., Nakajima, T., Honda, Y., Kitao, O., Nakai, H., Vreven, T., Montgomery, J. A., Jr., Peralta, J. E., Ogliaro, F., Bearpark, M., Heyd, J. J., Brothers, E., Kudin, K. N., Staroverov, V. N., Kobayashi, R., Normand, J., Raghavachari, K., Rendell, A., Burant, J. C., Iyengar, S. S., Tomasi, J., Cossi, M., Rega, N., Millam, J. M., Klene, M., Knox, J. E., Cross, J. B., Bakken, V., Adamo, C., Jaramillo, J., Gomperts, R., Stratmann, R. E., Yazyev, O., Austin, A. J., Cammi, R., Pomelli, C., Ochterski, J. W., Martin, R. L., Morokuma, K., Zakrzewski, V. G., Voth, G. A., Salvador, P., Dannenberg, J. J., Dapprich, S., Daniels, A. D., Farkas, Ö., Foresman, J. B., Ortiz, J. V. J. and Fox, D. J. (2016) Gaussian09 (Revision E). Wallington, USA: Gaussian Inc.

32. Jonuarti R., Wungu, T. D. K., Haryanto, F and Suprijadi (2018) DFT study on electronic structure and band decomposed charge density of the small rings zigzag boron nitride nanotubes. *APRN Journal of Engineering and Applied Sciences*, **13(24)**, 9542−9547.

Computational Density Functional Theory Investigation
of Stability and Electronic Structures on Boron Nitride
Systems Doped with/without Group IV Elements

33. Asif, F. B., Liakath Ali Khan, F., Muthu, S. and Raja, M. (2021) Computational evaluation on molecular structure (Monomer, Dimer), RDG, ELF, electronic (HOMO-LUMO, MEP) properties, and spectroscopic profiling of 8-Quinolinesulfonamide with molecular docking studies. *Computational and Theoretical Chemistry*, **1198**, 113169(1−20).

34. Muhammad, D., Matin, M. M., Miah, S. M. R. and Devi, P. (2021) Synthesis, antimicrobial, and DFT studies of some benzyl 4-O-acyl-α-L-rhamnopyranosides. *Orbital: The Electronic Journal of Chemistry*, **13(3)**, 250−258.

35. Rahman, M. A., Matin, M. M., Kumer, A., Chakma, U., Rahman, M. R. (2022) Modified D-Glucofuranoses as New Black Fungus Protease Inhibitors: Computational Screening, Docking, Dynamics, and QSAR Study. *Physical Chemistry Research*, **10(2)**, 189−203.

36. Bharathy, G., Prasana, J. C., Muthu, S., Irfan, A., Asif, F. B., Saral, A., Aayisha, S. and Devi, R. N. (2021) Evaluation of electronic and biological interactions between N-[4-(Ethylsulfamoyl)phenyl]acetamide and some polar liquids (IEFPCM solvation model) with Fukui function and molecular docking analysis. *Journal of Molecular Liquids*, **340**, 117271(1−14).